Journal of Applied Polymer Science

Preparation and Characterization of Bacterial Cellulose Microfiber/Goat Bone Apatite Composites for Bone Repair

Xiaoxia Fan,[1] Tingting Zhang,[1] Zhitong Zhao,[1] Haohao Ren,[1] Qiyi Zhang,[2] Yonggang Yan,[1] Guoyu Lv[1]

[1]College of Physical Science and Technology, Sichuan University, Chengdu 610064, China
[2]College of Chemical Engineering, Sichuan University, Chengdu 610064, China
Correspondence to: G. Lv (lgy929@126.com) or Y. Yan (yan_yonggang@vip.163.com).

ABSTRACT: Bacterial cellulose (BC) and goat bone apatite (GBA) composites were fabricated by a dissolving method. The 4-methylmorpholine-4-oxide (NMMO) served as the solvent for BC. Goat bone apatite was added to the NMMO solution of BC, so the shape of the material could be easily controlled by using appropriate molds. The expected composites were fabricated from NMMO by immersion in water-bath and formed by lyophilization. The results indicated that GBA was homogenously distributed into BC matrix and some interaction formed at the interface between BC and GBA. The crystallinity of BC in the composites decreased with the increase of GBA content. And the weight loss ratio of the composites decreased with the increase of GBA content and the degradation rate of BC/GBA composites could be adjusted by changing the GBA content in the composites. The surface, after soaking in PBS, was suitable for cell growth. The pH value of the medium was stable around 7.38 after the composites were immersed into PBS for 12 weeks, which was beneficial to bone cell differentiation. Furthermore, the MTT test results showed BC/GBA composites could stimulate cell proliferation and promote the cell differentiation. The results demonstrated that the prepared BC/GBA biocomposite could be a promising bone filler material for bone defects repair and construction. © 2012 Wiley Periodicals, Inc. J. Appl. Polym. Sci. 129: 595–603, 2013

KEYWORDS: biomaterials; biopolymers and renewable polymers; cellulose and other wood products; composites; degradation

Received 14 September 2012; accepted 8 October 2012; published online 9 November 2012
DOI: 10.1002/app.38702

INTRODUCTION

Bone is one of the most important biological structures in which nanometer-sized, poorly crystalline hydroxyapatite (HA) is distributed in and along the collagen fibers.[1–3] Congenital, hereditary, and unexpected events and traffic accidents can lead to bone damage and injury. To repair the damaged bone and to recover its biological function, various materials were developed to clinical application.[4–7] Among these materials, biocomposites, especially polymers combining with inorganic material showed advantages of both high bioactivity and biodegradability.[8–10] Compared to the synthetic polymer and chemical prepared HA, natural polymer and bone apatite possess better biocompatibility, biodegradability, microstructure and processability as well. For instance, bacterial cellulose (BC) was an attractive biomaterial for tissue engineering due to its biocompatibility, biodegradability[11–13] and 3D-microstructure,[14–18] which was similar to those hard and soft tissues and easily molded into a variety of shapes.[19–20] But single BC was rarely used as damaged bone repair materials because of its poor compatibility and lower bioactivity to bone tissue. BC composites were much better in the bone and other hard tissue repair and therapy, such as BC and hydroxyapatite nanocomposites had been studied for bone repair application.[21–22] Considering the biological behavior, the apatite calcined from animal bone showed more satisfactory results by repairing bone defection than that of synthesized hydroxyapatite.[23]

Considering the composition and biological property, the present research focused to develop a novel bacterial cellulose (BC)/goat bone apatite (GBA, calcined from goat bone) composite as fillers for bone and other hard tissue repairing and therapy. The combination of GBA and BC may result in a new bioactive material with good biological properties, biocompatibility, biodegradability and 3D-microstructure, which was similar to those hard and soft tissues and easily molded into a variety of shapes.

To achieve above aim, a series of BC/GBA composites had been prepared through the method of dissolving renewable technique and emulsion freeze-drying tech described in literature.[24–26] Therefore, in this study, dissolving renewable technique and characterization of BC/GBA composite were particularly discussed, and the *in vitro* degradability in phosphate buffered

Applied Polymer SCIENCE

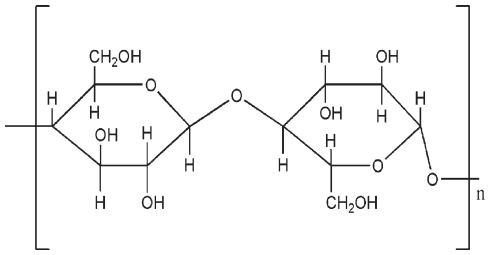

Scheme 1. The structure of cellulose.

saline (PBS) and cytotoxicity by MTT essay of BC/GBA composite were evaluated. The structure of cellulose and the possible bond of BC and goat bone apatite were designed as Schemes 1 and 2.

EXPERIMENTAL

Preparation of GBA (Goat Bone Apatite)

GBA (goat bone apatite) was calcined from fresh long tubular cortical bone of goat. Briefly, the fresh goat bone was collected and washed with water and ethanol. And then soft tissues were peeled and bone marrow was flushed out. Then the bone was crushed to granules using an axe and dried in the air. After that, then bone was gradually heated to 800°C and kept for 8 h in the furnace. After cooling to room temperature, the bone was ground into powder by using a mortar and collected to be used as the goat bone apatite for preparing BC/GBA composite.

Preparation and Characterization of BC/GBA Composites

The BC/GBA composites containing 30, 50, and 70 wt % of goat bone apatite labeled BC/GBA30, BC/GBA50, and BC/GBA70 were prepared by dissolving renewable method as previously described.[24] Briefly, 40 g NMMO, a small amount of water were added into the three-necked flask, then the BC was added into the dissolved NMMO and the mixture with strong stir was kept at 100°C for 4 h until BC was sufficiently dissolved. Different amount of goat bone apatite was added into three-necked flask, and then the mixture was kept at 100°C for another 1.5 h to mix sufficiently. After these, the products were cooled down to room temperature in selected molds. Then the products were soaked in deionized water at 40–50°C for 24 h to leach out the NMMO solvent. After immersion, the products were dried by freeze-drying technique, and the porous BC/GBA composites with different composition were finally obtained. The regeneration BC was prepared as a control sample using the same method.

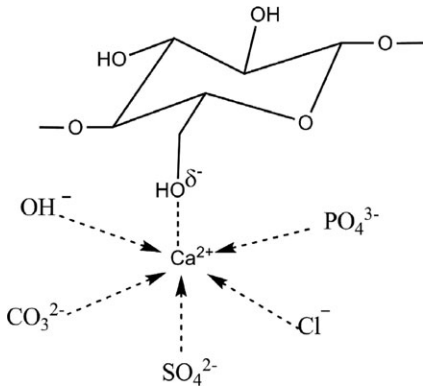

Scheme 2. The possible bond of cellulose and GBA.

Fourier transforms infrared (FTIR) spectroscopy spectra were conducted using a Perkin–Elmer 6000 FTIR spectrometer (Nicolet Perkin Elmer) to determine the structure of the composite with potassium bromide tabletting. XRD patterns of all the samples were recorded using a X-ray diffractometer (X'Pertpro-MPD) with Cu Kα radiation ($\lambda = 1.54$ Å) over the 2θ range of 10°–70°. X-ray photoelectron spectroscopy (XPS) was carried out with a XSAM800 (Kratos) Instrument. The morphology of BC/GBA composite was observed by scanning electron microscopy (SEM, JEOL JSM 5600LV, Japan) at 20 kV with gold-coating surface.

In Vitro Degradation of BC/GBA Composites

The test of biodegradation of pure BC, regeneration BC, and BC/GBA composites were carried out in phosphate buffered saline (PBS) solution (pH 7.4) at 37°C ± 0.2°C. BC and the various weight ratios of BC/GBA composites were immersed in 90 mg L^{-1} PBS solution. The PBS solution was renewed every 2 weeks. At predetermined time interval (2, 4, 6, 8, 10, and 12 weeks), the samples were taken out from the PBS solution, thoroughly rinsed with distilled water, dried in a vacuum oven for 8 h at 80°C, and weighed. The weight loss of the degradation was expressed as the percentage weight loss of the composites after treatment from three replicates as follow:

$$W = (W_0 - W_t)/W_0 \times 100$$

W, W_0, and W_t represent the percentage weight loss after PBS treatment, initial weight, and weight at time t, respectively. The weight loss values were expressed as the means with standard deviation ($n = 3$). The pH of the PBS medium after the samples soaking was recorded at each time point.

Cytotoxicity

L929 cells were used to evaluate the cytotoxicity of BC/GBA composites in this study, which have previously been widely employed as *in vitro* test for assessing the cytotoxicity of many types of biomaterials.[27] L929 cells proliferated at 37°C, 5% CO_2 in petri dishes (Φ100 mm) containing RPMI 1640 supplemented with 10% fetal bovine serum and antibiotics (100 U mL^{-1} penicillin, 100 μg mL^{-1} streptomycin). After growing nearly confluent, the cells were trypsinized, collected, and adjusted to 1×10^4 cells mL^{-1} for following experiment. Stirred cell suspension was pipetted into 96-well plate with 100 μL $well^{-1}$ which contained samples, incubated at 37°C, 5% CO_2. After these process, the samples for cell proliferation assay with MTT (MTT Kit, Roche Diagnosis, IN) were cultured after 1, 3, 5, and 7 days with a medium refreshing every 2 days. In brief, the supernatant in the 96-well was discarded and 50 μL MTT solution (1 mg mL^{-1}, dissolved in RPMI 1640 medium) was added into each well and incubated another 2 h at 37°C, 5% CO_2. RPMI 1640 (containing 10% FBS) were used as a control.

At the end of incubation, the supernatant in the 96-well was discarded, 100 μL of isopropanol was added and vortexed for 5 min to allow total color released from the bottom of 96-well

Table I. Criteria for Cytotoxicity Scoring

Grade	Reactivity	Condition of cultures
0	None	No detectable zone around or under specimen
1	Slight	Some malformed degenerated cells under specimen
2	Mild	Zone limited to area under specimen and up to 4 mm
3	Moderate	Zone extends 5–10 mm beyond specimen
4	Severe	Zone extends >10 mm beyond specimen

plate, the absorbency was measured at 570 nm by an enzyme-linked immuoadsorbent assay plate reader (reference wave length 650 nm). The cell viability percentage was calculated by comparing with the blanks (The cell viability percentage of the blanks represented as 100%). Six samples per time point per material were included. The results were reported as OD units and expressed as mean ± SD. Some samples were taken at day of 1, 3, and 5 for cell morphology assay. The criteria for cytotoxicity scores were shown in Table I.

RESULTS AND DISCUSSION

IR Analysis

The IR patterns of regenerated BC, GBA, and BC/GBA composites were shown in Figure 1. The bottom spectrum was a typical curve of regenerated BC, same as the pattern of pure BC as reported by Kim.[28] The absorption peak at 3200–3500 cm^{-1} was assigned to the hydroxyl group and hydrogen bond.[29] It can be seen that the specific peaks of GBA and BC appeared in the spectra of BC/GBA composites (as shown in Figure 1 and Table II) but with slight shifts. The peak around 3442 cm^{-1} of the OH^- group in BC became weak in composites and had some slight shifts as seen in Table II. The peaks at 1045 and 570 cm^{-1} were assigned to the characteristic stretching vibration peaks and bending vibration peaks of PO_4^{3-} in GBA, which had relative obvious changes in BC/GBA composites. The peaks at 1457 cm^{-1} were the characteristic peak of CO_3^{2-} and had some changes in composites. Additionally, the peaks of organic matter of H_2O were still found at nearly 1035 cm^{-1}. The peaks at 900 cm^{-1} were the characteristic peak of glycosidic band.[30] These transformations of characteristic absorption peaks might

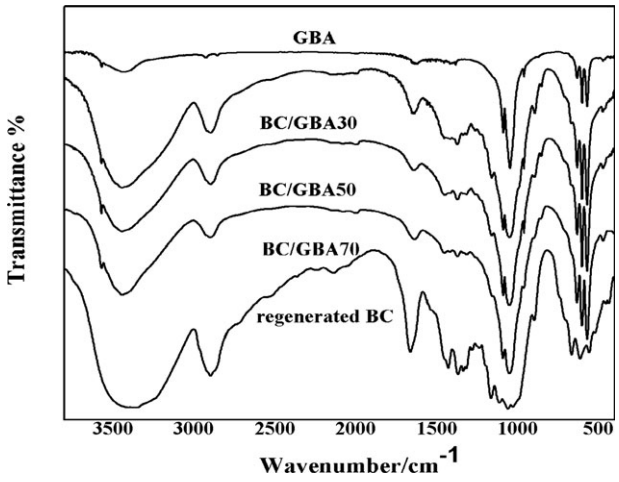

Figure 1. FT-IR spectra of regenerated BC, GBA, and BC/GBA composite with different GBA content.

be caused from the interface interaction between GBA and BC matrix. And from these changes, it could conclude that some new interface between GBA and BC formed.

XRD Analysis

The XRD patterns of regenerated BC, GBA, and BC/GBA composites were shown in Figure 2. The upper curve was a typical XRD pattern of regenerated BC, which was consistent with previous pure BC pattern.[31,32] The three peaks at $2\theta = 14.80°$, 17.05°, and 22.96° were belonged to the characteristic diffraction pattern of BC. The broad diffraction peaks observed for BC was due to the fact that BC was not a completely crystalline polymer.[33] The characteristic peaks of GBA appeared at $2\theta = 25.8°$, 31.7°, and 34.0°, the narrow diffraction peaks observed for GBA suggested that GBA had a high crystallinity. However, the crystallinity of GBA drastically decreased with the incorporation of BC (as seen in Figure 2). And the crystallinity of BC decreased with the increase of GBA content in the composites. The results indicated that the presence of GBA in the composite blocked the polymer chain close contact and leaded to the formation of more disordered polymer crystals characterized by more defected crystalline form. As a result, the BC into the BC/GBA composites showed lower crystallinity than that of pure BC. On the other hand, the results also revealed that the composites were composed of BC and GBA, and the synthesis of BC/GBA composites procedure did not change the composition of BC. The XRD analysis suggested that the crystallinity of BC decreased with the increase of GBA content, which might be

Table II. Characteristic Peak Shifts of Regenerated BC, GBA, and BC/GBA Composite with Different GBA Content

Characteristic peak shifts of IR	GBA (cm^{-1})	BC (cm^{-1})	BC/GBA30 (cm^{-1})	BC/GBA50 (cm^{-1})	BC/GBA70 (cm^{-1})
PO_4^{3-}/υ_3	1045.23	-	1053.04	1052.76	1052.29
PO_4^{3-}/υ_4	570.66	-	571.31	571.24	571.27
OH^-	3433.24	3442.57	3445.60	3445.79	3443.67
H_2O	1635.43	1635.68	1635.84	1635.52	1635.41
CO_3^{2-}	1457.28	-	1463.73	1463.69	1463.73

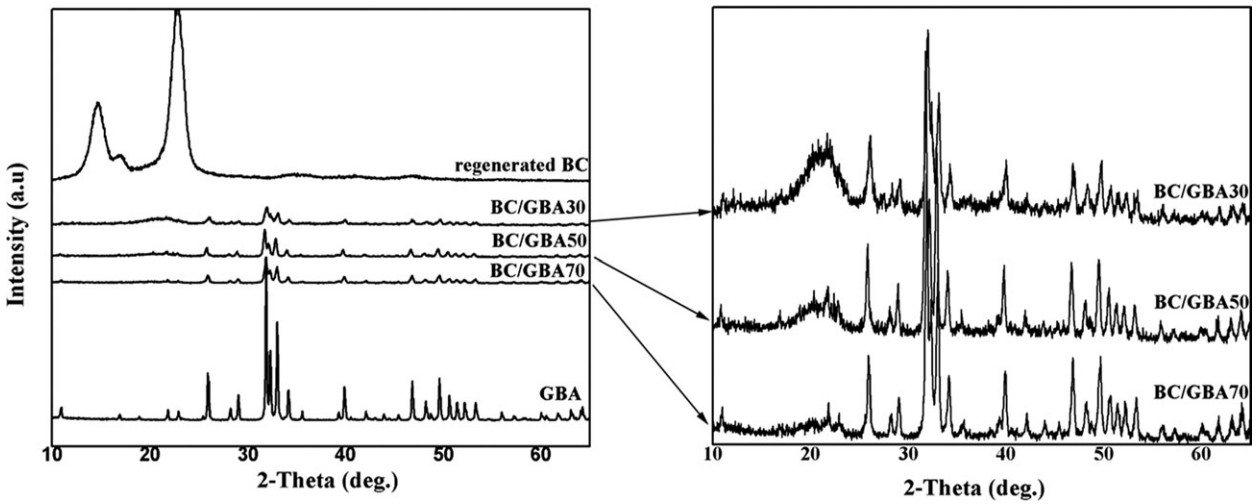

Figure 2. XRD patterns of regenerated BC, GBA, and BC/GBA composite with different GBA content.

caused by the interaction between GBA and BC at their interface. However, the detailed mechanisms governing this change are not yet fully understood. Further work is necessary to obtain more insights into the mechanisms.

XPS Analysis

XPS data (Figure 3) identified that carbon, calcium, oxygen, and silicon were the major elements of the BC/GBA composites. The binding energy of carbon, calcium, oxygen, and silicon of BC/GBA composites were shown in Table III.

Clearly, the binding energy of Ca_{2p} for BC/GBA (30, 50, 70) were lower than that of GBA by 0.1, 0.2, 0.4eV, respectively. It could be deduced that the Ca^{2+} (from GBA) in the composites was coordinated with both PO_4^{3-} and CO_3^{2-} as well as other ionic of GBA and the OH^- group in BC molecules. Therefore, it could be concluded that GBA combined with BC mainly by the formation of $OH^- \rightarrow Ca^{2+}$ linkage in the BC/GBA composites, which led to the decreasing of the Ca_{2p} binding energy in the composites.

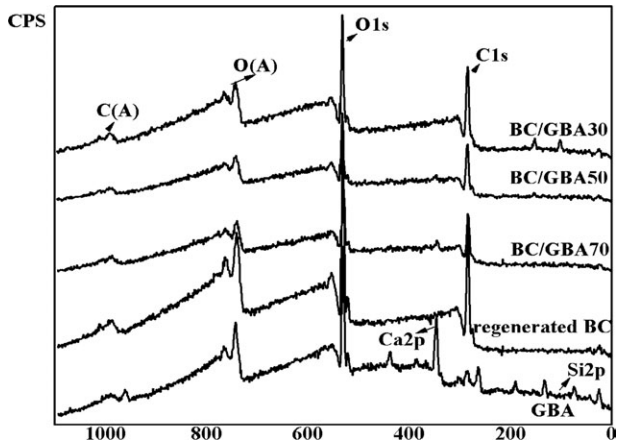

Figure 3. XPS patterns of regenerated BC, GBA, and BC/GBA composite with different GBA content.

O_{1s} binding energy at XPS spectra peak position was evaluated as 530.9, 530.7, 530.8, 531.2, and 531.1ev for BC, GBA, and BC/GBA 30, 50, 70, respectively. The results showed that the O_{1s} binding energy of the BC/GBA30, 50, 70 was higher than that of GBA by 0.1, 0.4, and 0.3 eV. When GBA was added to BC, the binding energy increased with the increase of GBA content, which might be attributed to the change of BC from oxide to ionic compound, and ionic bond was stronger than covalent bond in this substance, so the binding energy of O_{1s} for the composites was higher than that of GBA.

Si_{2p} binding energy at XPS spectra peak position was evaluated as 100.8, 101.1, 102, and 103 eV for BC/GBA30, 50, 70, and GBA, respectively. The results showed that the Si_{2p} binding energy of the BC/GBA (30, 50, 70) was lower than that of GBA by 2.2, 1.9, and 1.0 eV, respectively. When Si^{4+} in GBA was coordinated with OH^- in the BC, the organic bond Si—O in the BC/GBA was formed, so the binding energy of Si_{2p} for the composites was lower than that of GBA. From these facts, it could be drawn a conclusion that some interaction and new interface formed between GBA and BC, and the results of XPS was in accordance with the results of IR.

SEM Micrograph

Figure 4 shows the typical SEM images of surface morphology of regeneration BC and BC/GBA composite containing 50% (wt) GBA. Figure 5 shows the optical photograph of the BC/GBA50 composite. As seen in Figure 5(a,b), a well-organized

Table III. Binding Energy of Regenerated BC, GBA, and BC/GBA Composite with Different GBA Content

BE	C_{1s}	Ca_{2p}	O_{1s}	Si_{2p}
Regenerated BC	284.8	-	530.9	-
BC/GBA30	284.8	346.6	530.8	100.8
BC/GBA50	284.8	346.5	531.2	101.1
BC/GBA70	284.8	346.3	531.1	102
GBA	284.8	346.7	530.7	103.0

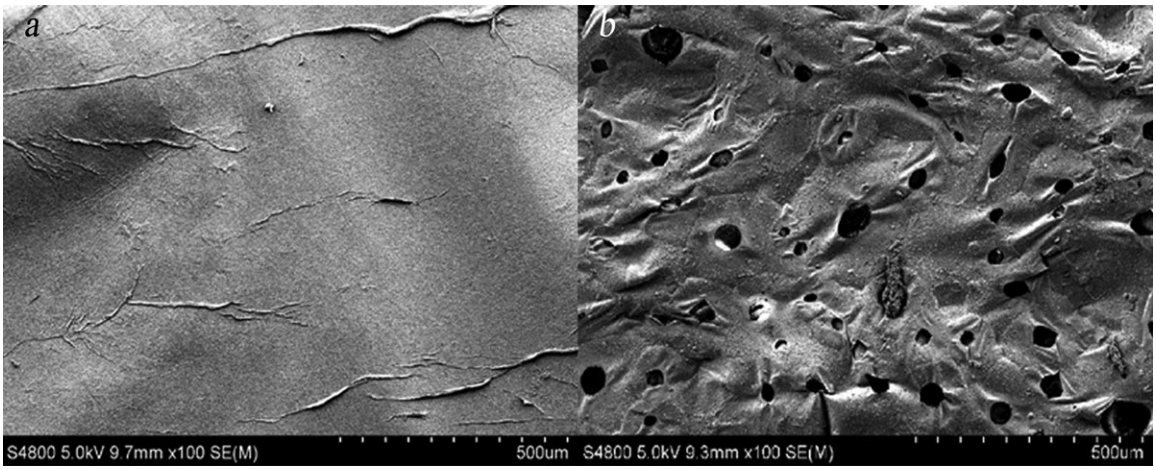

Figure 4. SEM patterns of regeneration BC and BC/GBA50 composite.

three-dimensional (3D) network structure was observed. Evidently, the BC/GBA composite were porous with honeycomb pores, which might be more in favor of cells interacting in the pore walls, and it would be promoting chondrogenic differentiation of the stem cells and chondrocytes phenotype maintenance. The SEM examinations of BC/GBA composite revealed that GBA was dispersed in the polymer matrix, and macroporous were found in the composite [Figure 4(b)]. There were no obvious pores found in regeneration BC [Figure 4(a)], which demonstrated that pores in the composite were caused by adding GBA into BC. And SEM micrograph also showed the homogenous surface of the BC/GBA composite.

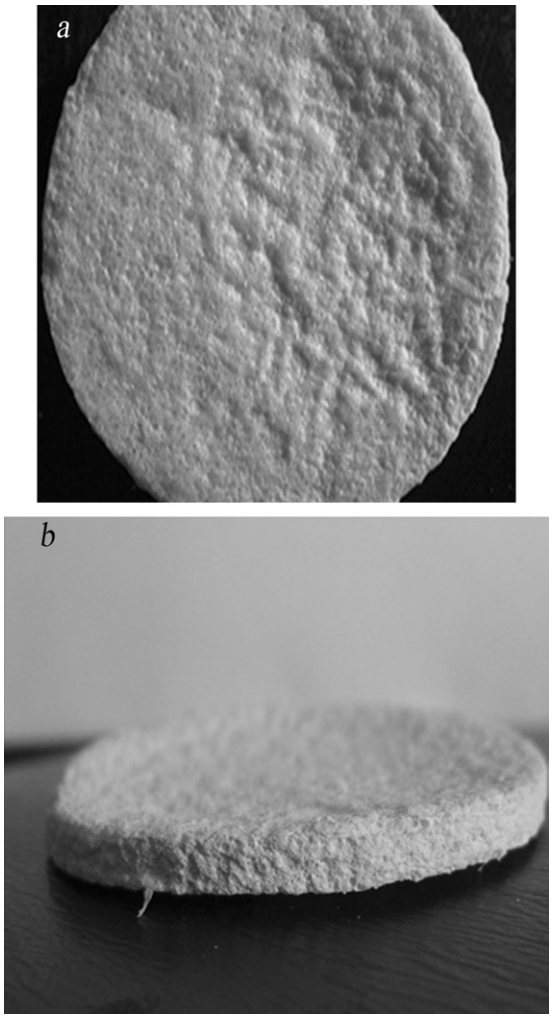

Figure 5. Optical photograph of BC/GBA50 composite.

In Vitro Degradation of BC/GBA Composites

Weight Loss in PBS. The weight loss ratios of regenerated BC and BC with different contents of GBA (30, 50, 70) as well as GBA were shown in Figure 6. The reliable weight loss of pure BC scaffold could not be obtained at the end of incubation because the dissociation of BC nanofibrils occurred during incubation period of 4 weeks. While renewable BC had a relative faster degradation rate (as 8.0% after 12 weeks) compared with GBA (1.7%). The weight loss of composites decreased slowly in the first 2 weeks, and then followed a relative rapid degradation rate after 4 weeks. After 12 weeks soaking time, the total weight loss of the 30, 50, 70% BC/GBA composites

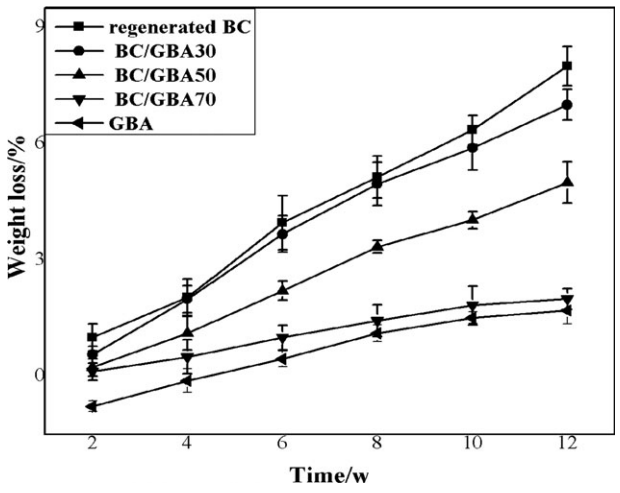

Figure 6. Weight loss of regenerated BC, GBA, and BC/GBA composite with different GBA content.

Applied Polymer SCIENCE

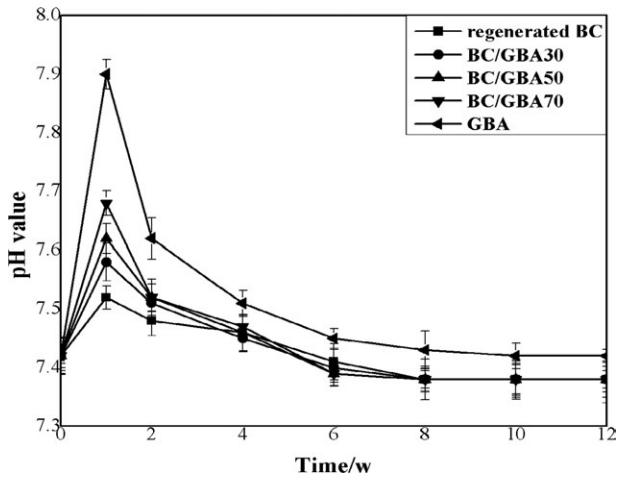

Figure 7. pH value variation of regenerated BC, GBA, and BC/GBA composite with different GBA content.

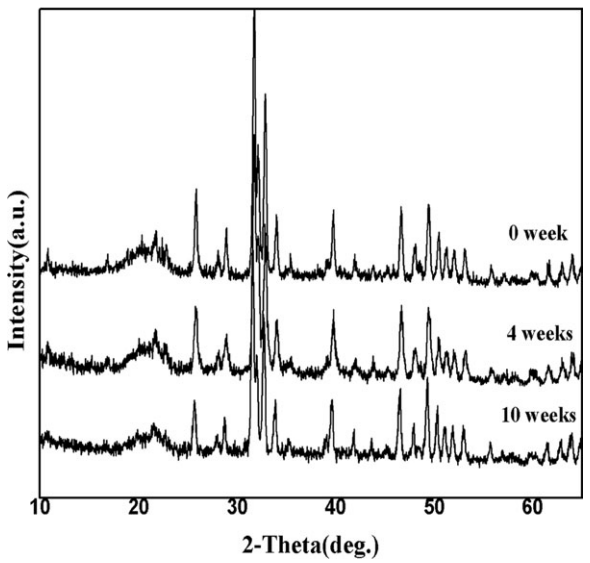

Figure 9. XRD patterns of BC/GBA50 composite after degradation for 0, 4, and 10 weeks.

reached around 7, 5, and 2%, respectively. The results demonstrated that the amount of GBA in the composites had obvious effects on the weight loss ratio of the BC/GBA composites. With the increase of the GBA content, the weight loss of composites decreased. This might be attributed to the interaction of surface between GBA and BC. As described in the previous literature, BC was a degradable material which had good degradability,[13–15] but there is no specific degradation figure in any literature. From the present results, it was found that the degradation rate of BC was low, and the degradation rate of BC/GBA composites could be adjusted by changing the GBA content in the composite.

pH Value Change of the Soaking Medium. The pH value variation of the medium after the samples soaking into PBS was shown in Figure 7. It was shown that the pH of regeneration BC had some changes in the PBS (from 7.52 to 7.38) and kept neutral at last. Comparably, the PBS solution of GBA showed an obvious pH change during the first 8 weeks from 7.90 to 7.42, which demonstrated that the content of the GBA had an evident influence on the composites. it is well known, relatively low or high pH may cause detrimental effects on the surrounding tissue, such as local cell morbidity and tissue necrosis during its implantation.[34] So, the pH of composites at different ratios varied from 7.68 to 7.38, indicating that the degradation products could have little effect on the acidity of the ambient environment, which might be not give rise to adverse response to tissue *in vivo*.

SEM Analysis of Degradation Materials

Figure 8 shows the typical SEM images of surface morphology of BC/GBA composite containing 50% (wt)GBA as seen in Figure 8(a), and its surface morphology of degradation after the fourth week and the tenth week as seen in Figure 8(b,c). It was shown that the surface of composite had obvious changes as time passed. Considering low degradation ratio of materials, it can be deduced that mechanism of degradation might be surface erosion. Evidently, with the surface of BC/GBA composite get rougher, it would be more in favor of cells interacting in the pore walls and promoting chondrogenic differentiation of the stem cells and chondrocytes phenotype maintenance.

XRD Analysis of Degraded Materials

The XRD patterns of BC/GBA composite containing 50% (wt) GBA were shown in Figure 9. The upper curve (0 week) was a XRD pattern of BC/GBA50 composite. The lower curve (10

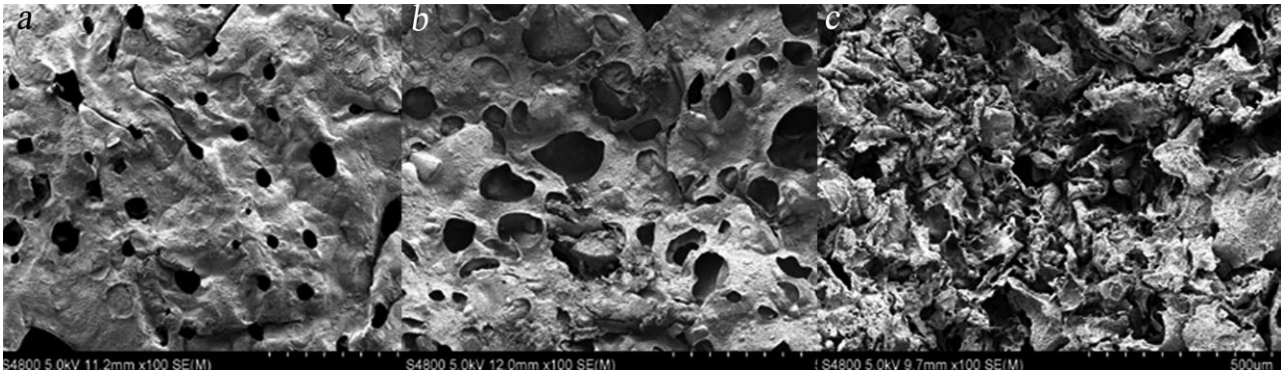

Figure 8. SEM morphologies of BC/GBA50 composite after degradation for 0, 4, and 10 weeks.

Table IV. The OD Values and Cytotoxicity Grade of Specimens by Extract Liquid with L929

Time	The blank one	BC			BC/GBA50		
	OD	OD	RGR (%)	Cytotoxicity	OD	RGR (%)	Cytotoxicity
1 day	0.094 ± 0.006	0.079 ± 0.011	84.04	1	0.098 ± 0.021	104.2	0
3 days	0.292 ± 0.008	0.245 ± 0.014	83.90	1	0.275 ± 0.012	94.18	1
5 days	0.882 ± 0.012	0.734 ± 0.023	83.22	1	0.874 ± 0.017	99.09	1
7 days	0.807 ± 0.015	0.779 ± 0.018	96.53	1	1.025 ± 0.023	127.0	0

weeks) was a degradation pattern of BC/GBA50 composite after 10 weeks. The middle curve (4 weeks) was a degradation pattern of BC/GBA50 composite after 4 weeks. It can be seen that the crystallinity of composite decreased slightly with extended immersion time. The characteristic diffraction pattern of BC at $2\theta = 14.80°$ and 17.05° and 22.96° decreased mildly and there was no obvious changes found in the characteristic diffraction of GBA. The results indicated that the composite degraded in very small extent, which were consistent with the degradation test of before.

Cytotoxicity

Proliferation of L929 cells on composites (BC as controls) was evaluated using the MTT assay because optical density (OD) values could provide an indicator for the cell viability on the biomaterials. It was found from Table IV that the OD value for the BC/GBA50 and BC increased significantly with the time, revealing that the L929 cells were able to proliferate on these samples, suggesting positive cellular responses to the BC/GBA50 composite and control (BC). To sum up, the test sample showed no evidence of causing cell toxicity and the grade was less than a grade 2 (mild reactivity), as compared with Table I.

The microscope images of the morphology of L929 cells cultured on BC/GBA50 at 1, 3, 5 days were shown in Figure 10(a–c), respectively. The blank group was shown in Figure 10(d–f) as control. It can be seen that the L929 cells differentiated well on BC/GBA50 as compared to blank one. From information above, it could conclude that the prepared BC/GBA composite was no obvious toxicity and could be suitable for implant *in vivo*.

FURTHER DISCUSSION

A common feature of biomaterials was that the interface and interaction had great influence on nature of materials.[35] In this research, GBA was compound with BC to form a novel biomaterial, the composites contained both properties of GBA and BC. Overall considering the results of IR, XRD, and XPS, it could be drawn a conclusion that strong interactions were present between the BC and GBA interface in the composites. Considering the composition of BC/GBA composite, the bone-like apatite in the composite sintered from goat bone, a natural apatite resource which has much similar composition to the human apatite, and has higher bioactivity than that of synthesized hydroxyapatite. Previous researcher[23] also found

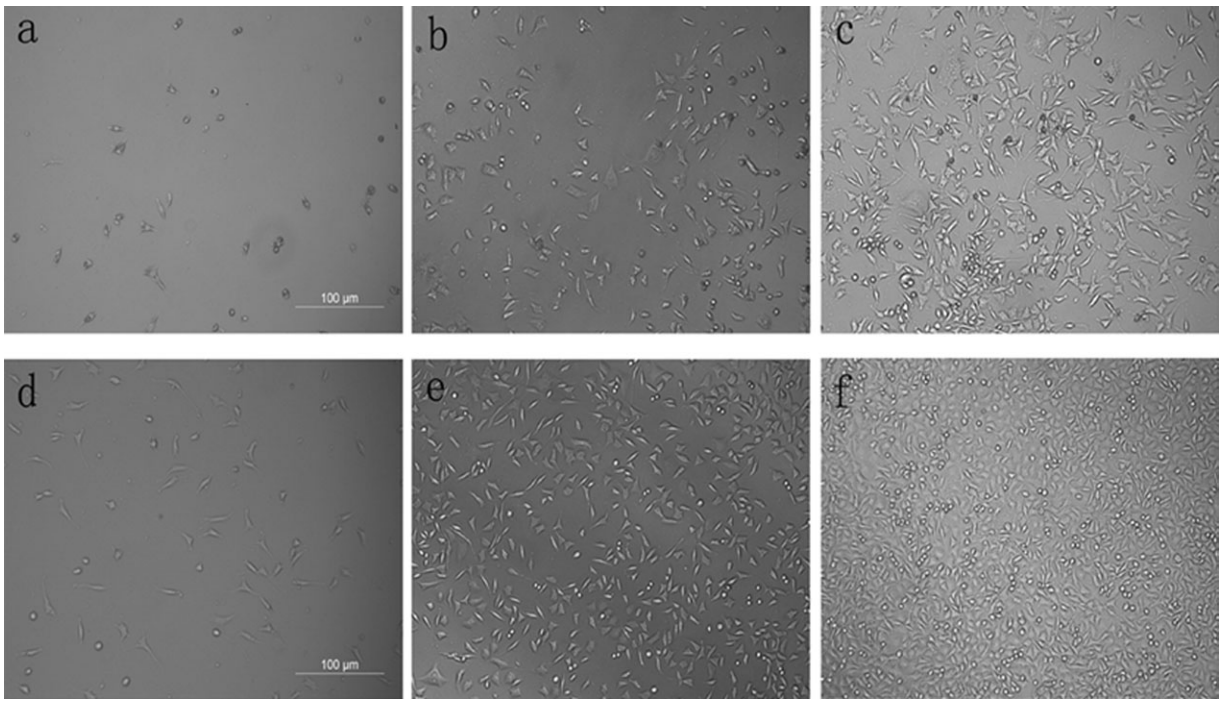

Figure 10. Morphologies of L929 cells on BC/GBA50 for 1, 3, and 5 days, blank group as control.

hyperthermia bone of animal was used as inorganic phase, which obtained satisfactory results by repairing bone defection.

Proper degradation ratio of bio-implants in the physiological environment is one of the most important characteristics of a biomaterial.[36] In this study, it was found that both GBA (1.7%) and BC (8.0%) exhibited slow degradation soaking in PBS. The weight loss ratio of the composites decreased with the increase of GBA content, which may be resulted from decreasing of hydrophilicity of BC by combined with GBA. But the degradation rate of BC/GBA composites could be adjusted by changing the GBA content in the composite. This property provided an alternative choice for the different degradation rate in the clinical application.

The pH value of the physiological environment after biomaterials implanted *in vivo* would greatly influence the interactions between cells and implants through cellular responses.[37] Some researches had shown that an acid environment (low pH) might be clinically undesirable and went against cell subsistence.[38] In this study, the results showed that the pH of the PBS solution decreased for BC/GBA composites from 7.62 to 7.38, and for BC from 7.52 to 7.38 at the first 8 weeks. The final pH value was stable at 7.38 for both BC/GBA composites and BC, which were very suitable for the cell growth.[39] Most studies suggest that weak basic environment be beneficial to bone cell differentiation and new bone formation. In view of this point, the prepared BC/GBA composites showed a good environment for bone regeneration.

Adding GBA into BC clearly improved biological properties of composites as well as cell proliferation. Previous studies had reported that ion dissolved products containing Ca and P from biomaterials could stimulate bone cell proliferation and differentiation.[40] In this research, the prepared new BC/GBA composites contained goat bone apatite, in which the Ca and P ions could release into the PBS solution, and could provide higher Ca and P ion when the BC/GBA composite was implanted into the bone tissue. The release of Ca and P ions from BC/GBA composite into tissue fluid might be responsible for stimulating cell proliferation and promoting the bone construction.

CONCLUSIONS

A novel BC/GBA biocomposite was prepared by using the dissolving regeneration method in this study. The GBA was homogenously distributed into BC matrix and some interaction formed at the interface between BC and GBA. The crystallinity of BC in the composites decreased with the increase of GBA content. Also, the weight loss ratio of the composites decreased with the increase of GBA content and the degradation rate of BC/GBA composites could be adjusted by changing the GBA content in the composites. The morphological surface after soaking in PSB was much suitable for cell growth. The pH value of the medium was stable around 7.38 after the composites immerged into PBS for 12 weeks, which was beneficial to bone cell differentiation. Furthermore, the MTT test results showed BC/GBA composites could stimulate cell proliferation and promote the cell differentiation. The results demonstrated that the prepared BC/GBA biocomposite could be a promising bone filler material for bone defects repair and construction.

ACKNOWLEDGMENTS

The authors are grateful for the financial support from National Key Technology R&D Program in the 11th Five Year Plan of China (NO. 2007BAE12B00).

REFERENCES

1. Rho, J. Y.; Kuhn-Spearing, L.; Zioupos, P. *Med. Eng. Phys.* **1998**, *20*, 92.
2. Olszta, M. J.; Cheng, X.; Jee, S. S.; Kumar, R.; Kim, Y. Y.; Kaufman, M. J.; Douglas, E. P.; Gower, L. B. *Mater. Sci. Eng.* **2007**, *58*, 77.
3. Bonakdarpour, A.; Reinus, W. R.; Khurana, J. S. Diagnostic Imaging of Musculoskeletal Diseases: A Systematic Approach; Springer Science+ Business Media, LLC, New York, **2010**. p 677.
4. Li, Y. B.; Rong, L. J.; Li, Y. Y. *Mater. Sci. Eng. A* **1998**, *255*, 70.
5. Huan, Z. G.; Chang, J. *Acta. Biomater.* **2009**, *5*, 1253.
6. Ruszczak, Z. *Adv. Drug Deliv. Rev.* **2003**, *55*, 1595.
7. Yang, Z.; Yuan, H.; Tong, W. *Biomaterials* **1996**, *17*, 2131.
8. Zhang, R.; Ma, P. X. *J. Biomed. Mater. Res.* **1999**, *44*, 446.
9. Wei, J.; Li, Y. B. *J. Eur. Polym.* **2004**, *40*, 509.
10. Yan, Y. G.; Li, Y. B.; Wei, J. *J. Eur. Polym.* **2003**, *2*, 411.
11. Czaja, W. K.; Young, D. J.; Kawecki, M.; Brown, R. M. *Biomacromolecules* **2007**, *8*, 1.
12. Klemm, D.; Schumann, D.; Udhardt, U.; Marsch, S. *Prog. Polym. Sci.* **2001**, *26*, 1561.
13. Czaja, W.; Krystynowicz, A.; Bielecki, S.; Brown, R. M. *Biomaterials* **2005**, *27*, 145.
14. Wippermann, J.; Schumann, D.; Klemm, D.; Kosmehl, H.; Salchigelani, S.; Wahlers, T. *Eur. J. Endovasc. Surg.* **2009**, *37*, 592.
15. Backdahl, H.; Esguerra, M.; Delbro, D.; Risberg, B.; Gatenholm, P. *J. Tissue Eng. Regen. Med.* **2008**, *2*, 320.
16. Chiaoprakobkij, N.; Sanchavanakit, N.; Subbalekha, K.; Pavasant, P.; Phisalaphong, M. *Carbohydr. Polym.* **2011**, *85*, 548.
17. Svensson, A.; Nicklasson, E.; Harrah, T.; Panilaitis, B.; Kaplan, D. L.; Brittberg, M.; Gatenholm, P. *Biomaterials* **2005**, *26*, 419.
18. Fang, B.; Wan, Y. Z.; Tang, T. T.; Gao, C.; Dai, K. R. *Tissue Eng. A* **2009**, *15*, 1091.
19. Risbud, M. V.; Bhonde, R. R. *J. Biomed. Mater. Res.* **2001**, *54*, 436.
20. Miyamoto, T.; Takahashi, S.; Ito, H.; Inagaki, H.; Noishiki, Y. *J. Biomed. Mater. Res.* **1989**, *23*, 125.
21. Zimmermann, K. A.; LeBlanc, J. M.; Sheets, K. T.; Fox, R. W.; Gatenholm, P. *Mater. Sci. Eng. C* **2011**, *31*, 43.
22. Hong, L.; Wang, Y. L.; Jia, S. R.; Huang, Y.; Gao, C.; Wan, Y. Z. *Mater. Lett.* **2005**, *60*, 1710.
23. Tatsuya, K.; Keiji, S.; Morio, K.; Hisashi, I.; Takayuki, M. *Clin. Orthop.* **1993**, *287*, 266.

24. Abe, Y.; Mochizuki, A. *J. Appl. Polym. Sci.* **2003**, *89*, 1671.
25. Yang, C.; Gao, C.; Wan, Y.; Tang, T.; Zhang, S.; Dai, K. *J. Porous Mater.* **2011**, *5*, 545.
26. Gao, C.; Wan, Y.; Yang, C.; Dai, K.; Tang, T.; Luo, H.; Wang, J. *J. Porous Mater.* **2011**, *18*, 139.
27. Hexig, B.; Nakaoka, R.; Tsuchiya, T. *J. Artif. Organs* **2008**, *11*, 204.
28. Kim, D. Y.; Nishiyama, Y.; Kuga, S. *Cellulose* **2002**, *9*, 361.
29. Choi, Y. J.; Ahn, Y.; Kang, M. S.; Jun, H. K.; Kim, I. S.; Moon, S. H. *J. Chem. Technol. Biotechnol.* **2004**, *79*, 79.
30. Grande, C. J.; Torres, F. G.; Gomez, C. M.; Troncoso, O. P. *Mater. Sci. Eng. C* **2009**, *29*, 1098.
31. Wan, Y. Z.; Hong, L.; Jia, S. R.; Huang, Y.; Zhu, Y.; Wang, Y. L.; Jiang, H. J. *Compos. Sci. Technol.* **2006**, *66*, 1825.
32. Toyosaki, H.; Naritomi, T.; Seto, A.; Matsuoka, M.; Tsuchida, T.; Yoshinaga, F. *Biosci. Biotechnol. Biochem.* **1995**, *59*, 1498.
33. Watanabe, K.; Tabuchi, M.; Morinaga, Y.; Yoshinaga, F. *Cellulose* **1998**, *5*, 187.
34. Chou, Y. F.; Chiou, W. A.; Xu, Y.; Dunn, J. Y.; Wu, B. M. *Biomaterials* **2004**, *25*, 5323.
35. Wilson, C. J.; Clegg, R. E.; Leavesley, D. I.; Pearcy, M. J. *Tissue Eng.* **2005**, *11*, 1.
36. Don, Z. H.; Li, Y. B.; Zou, Q. *Appl. Surf. Sci.* **2009**, *255*, 6087.
37. Richert, L.; Arntz, Y.; Schaaf, P.; Voegel, J. C.; Picart, C. *Surf. Sci.* **2004**, *570*, 13.
38. Yang, S. Y.; Mendelsohn, J. D.; Rubner, M. F. *Biomacromolecules* **2003**, *4*, 987.
39. Chaudhry, M. A.; Bowen, B. D.; Piret, J. M. *Biochem. Eng. J.* **2009**, *45*, 126.
40. Chen, Q. Z.; Efthymiou, A.; Salih, V.; Boccaccini, A. R. *J. Biomed. Mater. Res. A* **2007**, *84*, 1049.